Aerosol and Air Quality Research, 17: 3194–3208, 2017

ISSN: 1680-8584 print / 2071-1409 online
doi: 10.4209/aaqr.2017.01.0020

Comparison of Aerosol Hygroscopcity, Volatility, and Chemical Composition between a Suburban Site in the Pearl River Delta Region and a Marine Site in Okinawa

Mingfu Cai[1], Haobo Tan[2*], Chak K. Chan[3,4], Michihiro Mochida[5], Shiro Hatakeyama[6], Yutaka Kondo[7], Misha I. Schurman[3], Hanbing Xu[1], Fei Li[2], Kojiro Shimada[5], Liu Li[1], Yange Deng[5], Hikari Yai[5], Atsushi Matsuki[8], Yiming Qin[3], Jun Zhao[1*]

[1] *School of Atmospheric Sciences, Guangdong Province Key Laboratory for Climate Change and Natural Disaster Studies, and Institute of Earth Climate and Environment System, Sun Yat-sen University, Guangzhou, Guangdong 510275, China*
[2] *Institute of Tropical and Marine Meteorology/Guangdong Provincial Key Laboratory of Regional Numerical Weather Prediction, CMA, Guangzhou 510640, China*
[3] *Hong Kong University of Science and Technology, Hong Kong, China*
[4] *School of Energy and Environment, City University of Hong Kong, Hong Kong, China*
[5] *Nagoya University, Nagoya 464-8601, Japan*
[6] *Tokyo University of Agriculture and Technology, Tokyo 183-8059, Japan*
[7] *NIPR National Institute of Polar Research, Tokyo 190-0014, Japan*
[8] *Kanazawa University, Kanazawa 920-1192, Japan*

ABSTRACT

A suite of advanced instruments were employed to measure aerosol hygroscopicity, volatility and chemical composition at a suburban site in the Pearl River Delta (PRD) Region and at a marine site in Okinawa, respectively. The results showed that the particle number concentration in PRD is approximately ten times higher than that in Okinawa. Organics contributes about one half of the total NR-PM_1 concentration in PRD, while sulfate is the dominant component (about 60%) in Okinawa. Diurnal variation of the chemical species demonstrated that the site in PRD was affected by traffic-related sources and industrial emissions, while the one in Okinawa is mainly affected by regional emissions. The V-TDMA measurements showed that a large fraction (20–45%) of particles in Okinawa volatilized at about 200°C and nearly all particles volatilized at about 300°C, indicating that the particles were almost volatile in Okinawa. In contrast, a fraction (15–21%) of particles in PRD did not evaporate even when heated to about 300°C, implying that these particles might contain black carbon or low-volatile organics. For 40–200 nm particles in Okinawa, the hygroscopicity parameter κ is around 0.5, significantly higher than that of PRD particles ($\kappa \approx 0.26$). Particles tend to have bimodal distribution in PRD and unimodal in Okinawa, indicating that the former is externally mixed while the latter is internally mixed.

Keywords: Hygroscopicity; Chemical composition; Volatility; Pearl River Delta.

INTRODUCTION

Atmospheric particles can affect the climate system directly by scattering and absorbing solar radiation, or indirectly by changing the cloud lifetime and albedo (Randall *et al.*, 2007). The Intergovernmental Panel on Climate Change (IPCC 4th, 2013) suggested that both direct and indirect effects lead to net cooling in the atmosphere. However, our understanding of the climatic effects of atmospheric aerosols is far from complete and aerosol radiative forcing currently represents the highest uncertainties among all the radiative forcing components (Stocker, 2013).

Atmospheric particles can be emitted directly into the atmosphere (primary particles) or can be formed from their gaseous precursors or from heterogeneous reactions on preexisting particles (secondary particles). Both sizes and chemical composition matter for determining the physical and chemical properties of the particles (e.g., hygroscopicity, volatility, mixing state, chemical composition), which play essential roles in affecting the climate. The ability of particles for scattering and absorbing solar radiation mainly depends on aerosol hygroscopicity, mixing state, and chemical

* Corresponding author.
E-mail address: hbtan@grmc.gov.cn (H. Tan); zhaojun23@mail.sysu.edu.cn (J. Zhao)

composition. Likewise, whether particles could act as cloud condensation nuclei (CCN) also depends on the physical and chemical properties of the particles (Dusek *et al.*, 2006). Aerosol hygroscopicity describes the ability of particles to absorb water vapor from the ambient atmosphere under different moisture conditions. The Hygroscopicity Tandem Differential Mobility Analyzer (H-TDMA) is widely used to measure aerosol hygroscopicity through a growth factor, defined by the ratio of the diameter of particles after exposing to a certain humidity to the dry diameter of the particles (usually below 20% RH). By selecting a dry diameter of particles in the first DMA, then exposing them downstream to an air flow with a fixed humidity, growth factors of various sizes under different humidity conditions can be obtained through scanning the size distribution of exposed particles in the second DMA. Measurements from H-TDMA can also infer aerosol mixing state, providing additional information on the aerosol properties. Aerosol volatility, which is a parameter highly-correlated with carbonaceous particles, describes how aerosol volatilizes under different temperatures and provides a quantitative description of aerosol mixing state and to a lesser extent, the degree of aging (usually denotes as NF_{LV}). Laboratory and field measurements have shown that aerosol hygroscopicity and volatility are correlated with chemical composition of the particles, which is related to the emission sources (Wehner *et al.*, 2004; Swietlicki *et al.*, 2008; Yeung *et al.*, 2014). An improved understanding of aerosol properties is hence needed in order to reduce the uncertainty of the aerosol effects in the climate modeling system under different emission scenarios.

The physical and chemical properties of atmospheric particles can vary substantially at regional scales due to different emission sources and meteorological conditions. They are also affected by transport that brings different air masses into the receptor area, potentially modifying aerosol properties in the region. Previous field measurements have shown that aerosol chemical composition can be very different under different emission regions which include urban, forest, and marine. Aerosol particles, especially $PM_{2.5}$, were usually dominated by organics matters in urban environments in China (Ye *et al.*, 2003; Yang *et al.*, 2005; Wang *et al.*, 2006; Tao *et al.*, 2013; Li *et al.*, 2014). In forest environments, aerosol chemical composition could differ by wind directions or measurement sites and the dominate species could be organics or sulfate (Allan *et al.*, 2006; Cavalli *et al.*, 2006; Li *et al.*, 2010). Marine aerosols were affected by anthropogenic emissions and their chemical composition could vary with different sources and locations (Heintzenberg *et al.*, 2000; Bardouki *et al.*, 2003). However, there were few studies about the aerosol hygroscopcity and volatility, particularly the differences of those properties between mega cities and remote regions in China (Wehner *et al.*, 2009; Liu *et al.*, 2011; Ye *et al.*, 2011; Tan *et al.*, 2013a; Cheung *et al.*, 2016).

In this study, we carried out field measurements at a suburban site in Guangzhou in China and a marine site in Okinawa in Japan. Guangzhou is located at the center of the Pearl River Delta (PRD), together with its surrounding cities, constituting of a mega city cluster in southern China. PRD is one of the fast economical growing regions in China and has been subjected to severe hazes and other photochemical pollution in the past decades (Chan and Yao, 2008). Guangzhou represents urban air pollution that is constrained by emission sources from coal-fired power plants, industries, transportation sectors, etc. In contrast, the marine site, located in Cape Hedo, at the northern end of Okinawa Island, is surrounded by ocean and less influenced by local anthropogenic emissions. Aerosols in Cape Hedo hence represent marine origin or transport from long distance. The measurements were performed in November during which photochemistry is still intensive and haze days occur frequently in Guangzhou. The measurements at the two sites improve our understanding on the differences of aerosol properties under different emission sources and implication for long range transport between the two locations. The H/V-TDMA (Hygroscopicity and Volatility Tandem Differential Mobility Analyzer) and Aerodyne high resolution time-of-flight aerosol mass spectrometer (HR-ToF-AMS) were employed to measure hygroscopicity, volatility, and chemical composition respectively. The relationship between aerosol hygroscopicity and chemical composition was studied based on the measurements. Mixing states of the aerosol particles were also investigated at the two sites and potential transport mechanisms were elucidated by the histories of the air masses during the measurements.

EXPERIMENTAL AND DATA ANALYSIS

Measurement Sites

The field experiments were conducted at the Chinese Meteorological Administration (CMA) Atmospheric Watch Network (CAWNET) Station in Panyu, Guangzhou, China and at the Hedo Station Observatory (HSO) in Cape Hedo, Okinawa, Japan, respectively. The Panyu suburban site is located at the top of Dazhengang Mountain (23°00'N, 113°21'E) with an altitude of about 150 meter. No significant local emission sources were found near the site. However, the site is largely impacted by urban pollution from downtown Guangzhou. The measurements were made in November 2014. During the measurement period, the Panyu site was mainly affected by north, east and southeast wind. The average wind speed and temperature were 1.1 m s^{-1} and 21.6°C, respectively. The Cape Hedo Station is located at the Northernmost of Okinawa main island (26°87'N, 128°25'E) with an altitude of about 60 meter. The station is mainly surrounded by the ocean without any significant local emission sources. The measurements were carried out during November 1–9, 2015. During the campaign, the measurement site was mainly affected by north and east wind. The average wind speed and temperature were 3.8 m s^{-1} and 24.0°C, respectively.

Measurements Hygroscopicity and Volatility

A hygroscopicity/volatility tandem differential mobility analyzer (H/V-TDMA) was employed to measure size-resolved aerosol hygrosocpicity, volatility and particle number size distribution (PNSD). The instrument was self-

developed by the Guangzhou Institute of Tropical and Marine Meteorology (ITMM) (Tan *et al.*, 2013b) and upgraded to include both H- and V-mode, instrumentation and algorithm (Cheung *et al.*, 2016). Here only configuration relevant to the measurements was described. The instrument was equipped with a $PM_{1.0}$ cyclone inlet. Sampling flow was first drawn through a Nafion dryer (Model PD-70T-24ss, Perma Pure Inc., USA) to achieve a RH of less than 10% at the exit of the dryer (particles are considered to be dried under this RH condition). The dried particles were subsequently charged through a neutralizer (AM^{241}) and selected by the first Differential Mobility Analyzer (DMA1, Model 3081L, TSI Inc.). The selected particles were then assigned to either the H- or V-mode controlled by a three-way solenoid valve after exiting the first DMA as respectively described below.

During the H-mode measurements, the selected particles of a specific diameter (D_0) (from DMA1) were introduced into a Nafion humidifier (Model PD-70T-24ss, Perma Pure Inc., USA) to achieve 90% RH (Guangzhou) or 85%RH (Cape Hedo) equilibria. A second differential mobility analyzer (DMA2, Model 3081L, TSI Inc.) and a condensation particle counter (CPC, Model 3772, TSI Inc.) were used to measure the number size distribution of the humidified particles (Dp). The RH dependent hygroscopic growth factor (HGF) at a certain dry diameter is then defined as:

$$HGF\left(RH, D_0\right) = \frac{Dp\left(RH\right)}{D_0} \quad (1)$$

In this mode, five dry electrical mobility diameters (40, 80, 110, 150, and 200 nm) were chosen, covering both Aitken mode and accumulation mode of particles. Standard polystyrene latex spheres (PSL) and ammonium sulfate were used to perform regular particle size calibration for the instrument.

In the V-mode measurements: compared to H-mode, one additional particle size (300 nm) was included so that six dry electrical mobility diameters (40, 80, 110, 150, 200, and 300 nm) were selected in the measurements. The selected particles from DMA1 were sequentially heated in a heated tube. Similar to the H mode, the number size distribution of the heated particles were measured by DMA2 and the downstream CPC. The temperature dependent volatility shrink factor (VSF) at a certain dry diameter is defined as:

$$VSF\left(T, D_0\right) = \frac{Dp\left(T\right)}{D_0} \quad (2)$$

Overall, it took around 3 h to complete a cycle of measurements that consisted of PNSD scans, H-mode measurements at preset RH and V-mode measurements at 25, 100, 200, and 300°C. At each temperature (or RH), the sampling time for six (or five) selected diameters from DMA1 took about half an hour and PNSD scans were made in-between.

Chemical Composition

Size resolved non-refractory PM_1 ($NR\text{-}PM_1$) composition was measured by an Aerodyne HR-ToF-AMS at the Panyu site. Here only a brief description relevant to the measurements is given. A full description of the instrumentation can be found elsewhere (Jimenez *et al.*, 2003; Decarlo *et al.*, 2006). The instrument was operated in three modes (pToF, V, and W mode). Particle size information can be obtained based on time-of-flight of the particles in pToF mode, corresponding to the aerodynamic diameter. In V and W modes, the resolving power of the mass spectrometer is approximately 2000 and 4000, respectively. The instrument collected alternatively 5-min average mass spectra for the V + pToF modes and the W mode. The ionization efficiency (IE) calibrations were performed weekly with the DMA size-selected (mobility diameter, D_m = 400 nm) pure ammonium nitrate particles. Background signals were obtained daily for about 30 minutes by introducing filtered ambient air with a HEPA filter in the sample flow. Prior to and at the end of the measurement period, flow rates were calibrated with a Gilian gilibrator and PSL particles (Duke Scientific, Palo Alto, CA, USA) and ammonium nitrate particles in the range of 178–800 nm were used to calibrate the pToF size. A more detailed description of the AMS performance during the measurements can be found in Qin *et al.* (2017).

Another Aerodyne HR-ToF-AMS was deployed at the Cape Hedo site. The instrument was operated in V + pToF mode (from m/z 8 to 214) and W mode (from m/z 2 to 556) alternatively, with a time resolution of 30 min. The IE calibrations and the flow rate calibration follow a similar procedure as described for the Panyu measurements. The pToF size calibration was performed using standard particles in six sizes (Thermo Scientific 3000 series, 100 nm, 200 nm, 300 nm, 500 nm, 700 nm, 900 nm) prior to the measurements. Baseline correction was done by sampling ambient filtered air with a HEPA filter three times during the measurement period.

During the measurement periods, the mass concentrations for particles below 100 nm were too low in both Guangzhou and Cape Hedo and we only consider here the chemical composition for particles larger than 100 nm.

Data Processing and Methodology

Hygroscopicity and Volatility Data

The measured probability density function (PDF) of the hygroscopic growth factors (HGF) and the volatility shrink factors (VSF) can deviate from the measured particle probability density function (denoted as HGF-PDF and VSF-PDF respectively hereafter). We used the TDMAfit algorithm (Stolzenburg and McMurry, 2008) to fit the HGF-PDF and VSF-PDF following the procedure below: the measured PDF was fitted with a superposition of one or more lognormal distribution functions by varying the mean HGF or VSF, standard deviation and number fraction in each lognormal mode until the measured PDF was reproduced. The HGF-PDF and VSF-PDF was fitted through the forward function that is dependent on the flow rate, DMA size parameters, and particle diameter (Stolzenburg

and McMurry, 2008).

The hygroscopicity parameter κ was calculated according to κ-Köhler theory (Petters and Kreidenweis, 2007), based on the hygroscopicity growth factor (HGF), relative humidity (RH), and the properties of the aerosols:

$$\kappa = \left(\mathrm{HGF}^3 - 1\right)\left(\frac{1}{\mathrm{RH}}\exp\left(\frac{4\sigma_{s/a}\mathrm{M_w}}{\mathrm{RT}\rho_w \mathrm{D}} - 1\right)\right) \quad (3)$$

where HGF is the hygroscopic growth factor, ρ_w is the density of water (about 998.234 kg m^{-3} at 293K), M_w is the molecular weight of water (0.018 kg mol^{-1}), $\sigma_{s/a}$ is the surface tension coefficient between water and air (about 0.0728 N m^{-1} at 293K), R is the universal gas constant (about 8.31 J mol^{-1} K^{-1}), T is temperature (in Kelvin), and D is the droplet diameter (in meter). The κ probability density function (κ-PDF), denoted as c(κ), was normalized, that is, $\int c(D_0,\kappa)d\kappa = 1$, for κ-PDF of particles with dry diameter D_0.

The hygroscopicity and volatility of aerosol particles (the ensemble mean κ_{mean}) can be alternatively evaluated by the equation below:

$$\kappa_{mean} = \int_0^\infty \kappa c\left(\kappa, D_0\right) d\kappa \quad (4)$$

the κ_{mean} is defined as number weighted mean growth factor of the κ-PDF over the whole κ range.

We categorized particles according to their κ or VSF values (Table 1). NF_{LH}, NF_{MH}, NF_{HV}, NF_{MV} and NF_{NV} denote the number fraction of Less-hygroscopic (LH), More-hygroscopic (MH), High-volatile (HV), Medium-volatile (MV) and Non-volatile (NV) group particles. This classification is different from the five- or three modes of particles we discussed in the following section which are based upon the emission sources of the particles.

Aerosol Hygroscopicity Prediction

In order to predict aerosol hygroscopicty based on chemical composition, the Zdanovskii, Stokes and Robinson (ZRS) (Zdanovskii, 1948; Stokes and Robinson, 1996) was applied:

$$\kappa = \sum_i \varepsilon_i \kappa_i \quad (5)$$

where ε_i is the volume fraction of each compound in the particles, κ_i is the κ value of each compound.

The AMS only provides the information of ion concentrations during the measurements, while the ZSR rules requires the volume fraction and hygroscopicity of each compound. A simplified ion pairing scheme developed by Gysel *et al.* (2007) was used to reconstruct five chemical species:

$$\begin{aligned}
n_{NH_4NO_3} &= n_{NO_3^-} \\
n_{H_2SO_4} &= \max\left(0, N_{SO_4^{2-}} - n_{NH_4^+} + n_{NO_3^-}\right) \\
n_{NH_4HSO_4} &= \min\left(2n_{SO_4^{2-}} - n_{NH_4^+} + n_{NO_3^-}, n_{NH_4^+} - n_{NO_3^-}\right) \\
n_{(NH_4)_2SO_4} &= \max\left(n_{NH_4^+} - n_{NO_3^-} - n_{SO_4^{2-}}, 0\right) \\
n_{HNO_3} &= 0,
\end{aligned} \quad (6)$$

where n denotes the number of moles. ADDEM (Topping *et al.*, 2005) was used in this study to calculate the κ values of inorganics compounds. The κ value of organics was assumed to be 0.1 (Meng *et al.*, 2014). The κ values of the related compounds in the study are listed in Table 2.

Back Trajectory Analysis and Air Mass Classification

The physical and chemical properties of atmospheric particles are closely related to the origin of the air masses. Here we employed Hybrid Single Particle Lagrangian Integrated Trajectory (HYSPLIT) to investigate the influences of air mass origin on aerosol hygrosocpicity, volatility and chemical composition using Global Data Assimilation System (GDAS) 1° global meteorological data as input parameters. The 72 hour back trajectories were calculated every 6 hour arriving at an altitude of 150 meter above mean sea level at the Panyu site and 60 meter above mean sea level at the Cape Hedo site, respectively. The cluster analysis was based on the results from the spatial distribution of the backward trajectories.

RESULTS AND DISCUSSION

Characterization of Aerosol Properties

Characteristics of Particle Number Size Distribution

The characteristics of the particles number size distributions (PNSD) are distinctly different between particles measured at the Panyu site (Guangzhou) and those at the Cape Hedo site (Okinawa) due to their different emission sources and precursors. Fig. 1 shows the average PNSD in Guangzhou and in Cape Hedo, along with lognormal peak fits. The fit based on the five modes in Guangzhou agree excellently with the measured PNSD, while the fit with the three modes in Cape Hedo is not as good as that in

Table 1. Classification of particles based on hygroscopicity and volatility.

Aerosol Property	Values	Classification
Hygroscopicity (κ)	< 0.2	Less-hygroscopic particles (LH)
	> 0.20	More-hygroscopic particles (MH)
Volatility (VSF)	< 0.4	High-volatile particles (HV)
	0.4–0.9	Medium-volatile particles (MV)
	> 0.9	Non-volatile particles (NV)

Table 2. The κ values of the related compounds.

Species	κ
NH_4NO_3	0.58
NH_4HSO_4	0.56
H_2SO_4	0.90
$(NH_4)_2SO_4$	0.48
Organics	0.10

Guangzhou, showing a slight deviation from the measured PNSD. The total particle number concentration (N_{CN}) in Guangzhou (averaged over the whole measurement period) is about 11400 # cm^{-3}, about 10 times that in Cape Hedo (1100 # cm^{-3}), indicating severe air pollution in urban Guangzhou, as compared to relatively clean marine atmosphere in Cape Hedo.

The average PNSD of Guangzhou exhibits a nucleation mode, two Aitken modes and two accumulation modes. These five mode peaks centered at about 10, 25, 70, 102 and 220 nm. However, the mean PNSD of Cape Hedo shows a nucleation mode (a peak centered at about 20 nm), an Aitken mode (a peak centered at about 50 nm) and an accumulation mode (a peak centered at about 106 nm). The differences of the particle mode distribution between the two measurement sites indicate that Guangzhou is affected by more complex emission sources than Cape Hedo, leading to the presence of both fresh and aged particles.

Characteristics of Aerosol Hygroscopicity and Volatility

Fig. 2 shows the differences of the κ_{mean} values for particles in Guangzhou and in Cape Hedo. The κ_{mean} values increased with particle sizes in Guangzhou from 0.22 for 40 nm particles to 0.31 for 200 nm particles, while they are relatively size independent (0.48–0.52) in Cape Hedo. The κ_{mean} in Cape Hedo was similar to that of the earlier measurements at the same site (Mochida *et al.*, 2010).The higher κ_{mean} values indicate that particles in Cape Hedo are more hygroscopic than those in Guangzhou, due likely to the differences in chemical composition. Particles in Guangzhou were dominated by organics, while particles in Cape Hedo were dominated by sulfate for particles larger than 200 nm and ammonium for particles smaller than 200 nm. The high mass fraction of sulfate and ammonium could lead to higher hygroscopicity.

Fig. 3 shows the average HGF-PDF at RH = 90% and VSF-PDF at 300°C for particles in Guangzhou and Cape Hedo respectively. The HGF-PDF for particles in Guangzhou tends to be bimodally distributed with one mode located around Gf = 1.0 (less-hygroscopic mode, LH) and the other around Gf = 1.4–1.6 (more-hygroscopic, MH), implying that particles in Guangzhou are more likely to be externally mixed. The peaks of the MH mode shift slightly to higher Gf for larger particles between 40 nm and 200 nm. In contrast, the LH mode moves distinctly to smaller Gf for larger particles.

The VSF-PDFs for particles in Guangzhou also exhibit bimodal patterns, with one non-volatile (NV) and one medium-volatility (MV) or high-volatility (HV) group for all particle sizes. The NV group particles become more distinct for larger particles. The bimodal behaviors for both HGF-PDF and VSF-PDF demonstrate that particles in Guangzhou are more likely to be externally mixed, with larger particles being more externally mixed than smaller particles. LH and/or NV group particles usually contain fresh black carbon (BC) and some organic matters (Cheung *et al.*, 2016), which are hydrophobic or refractory, while those with MH and/or HV or MV mainly contain inorganic salts.

The particles in Cape Hedo, on the other hand, exhibit

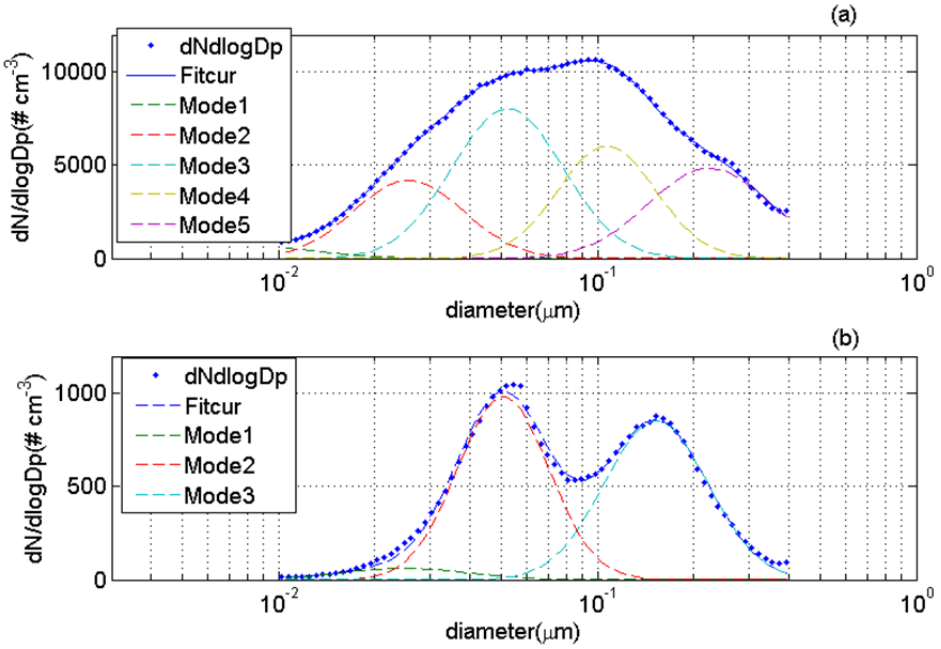

Fig. 1. The average particle number size distribution (PNSD) in Guangzhou (a) and in Cape Hedo (b) along with lognormal peak fits (five modes for Guangzhou and 3 modes for Cape Hedo).

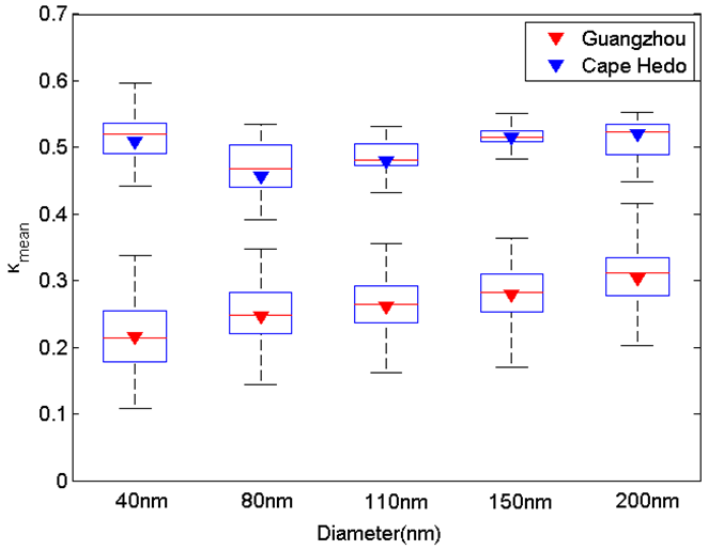

Fig. 2. The mean (± std) size-resolved κ (κ_{mean}) values of atmospheric particles in Guangzhou and Cape Hedo (shaded areas indicate the uncertainties of the κ_{mean} values).

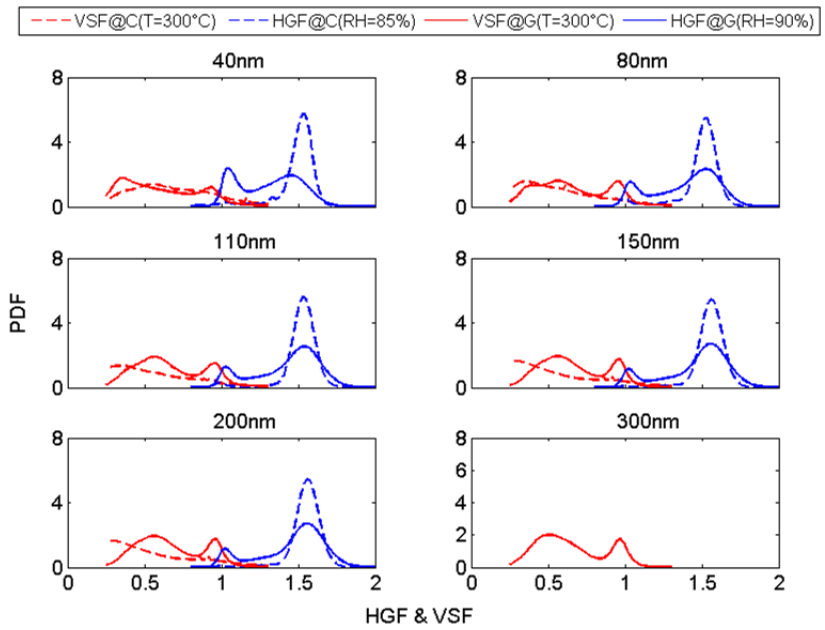

Fig. 3. The average HGF-PDFs (RH = 90%) (blue solid lines and blue dashed lines) and VF-PDFs (T = 300°C) (red solid lines and red dashed lises) for atmospheric particles in Guangzhou and Cape Hedo. C represents Cape Hedo and G represents Guangzhou.

bimodal features for HGF-PDF and unimodal for VSF-PDF. Only MH group particles were observed in Cape Hedo, suggesting that no externally mixed BC was found in ambient air in Cape Hedo. In addition, the MH mode does not shift toward higher Gf for larger particles as opposed to that in Guangzhou. A dominant MV mode was seen for VSF-PDF for all particle sizes with a VSF value of 0.2–0.3. Note that there is a small but distinct NV mode for VSF-PDF for particles larger than 80 nm, a small fraction of externally mixed particles that are attributed to refractory organics. It also implies that particles in Cape Hedo are regionally well distributed and aged rather than locally emitted, while particles in Guangzhou are affected by local emissions and the aged particles are well separated from the freshly emitted counterparts.

Figs. 4 and 5 compare the VSF-PDFs for six particle sizes at four temperatures in Guangzhou and in Cape Hedo, respectively. The VSF-PDF for particles in Guangzhou was characterized by a unimodal pattern at lower temperatures (25–100°C), implying that this fraction of particles can be evaporated below 100°C and volatility decreases as particle size increases. They can be attributed to nitrate or some highly (or semi-) volatile organics. The VSF-PDF exhibits a bimodal pattern at high temperatures (200–300°C) with a

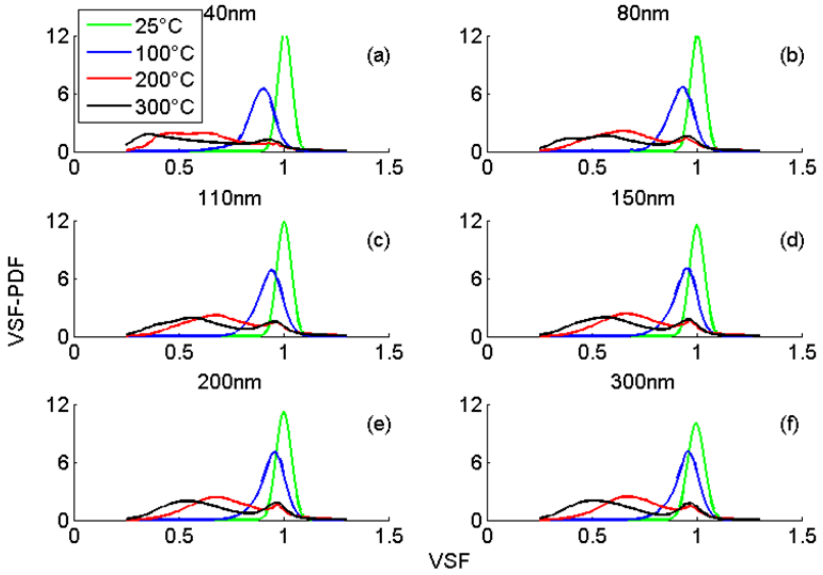

Fig. 4. The average VSF-PDF at four temperatures and six diameters for particles in Guangzhou.

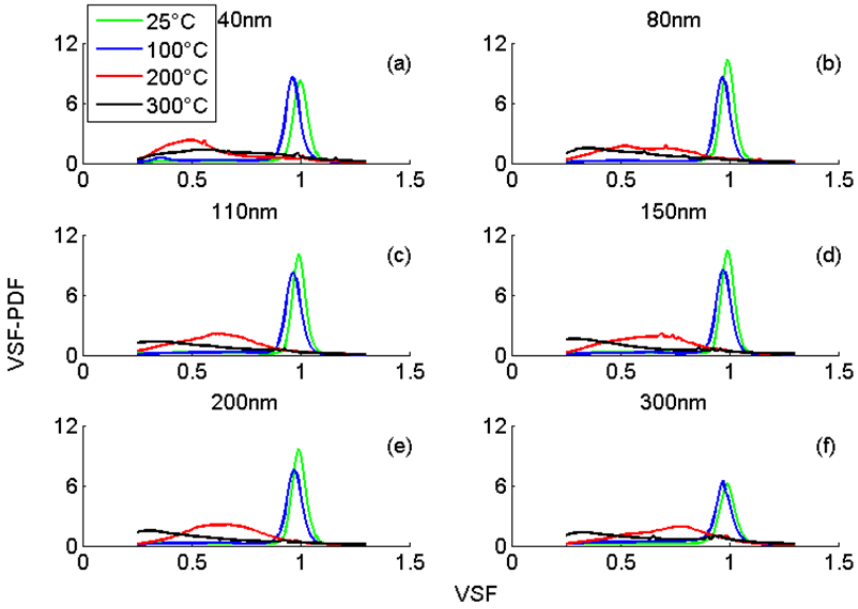

Fig. 5. The average VSF-PDF at four temperatures and six diameters for particles in Cape Hedo.

small but distinct NV mode and a significant MV or HV mode. The NV mode corresponds to a peak at VSF = 0.95–1, implying that these particles contain non-volatile species, probably black carbon (BC) or refractory organics. On the other hand, the MV mode corresponds to a peak at VSF = 0.5–0.7 at 200°C and slightly shifts to lower VSF values (HV mode) at 300°C, implying that these particles might contain predominantly sulfate (Wehner *et al.*, 2009; Cheung *et al.*, 2016).

The VSF-PDF for particles in Cape Hedo, however, shows exclusively unimodal with a NV mode observed for all sizes at a temperature below 100°C, implying that the particles contain a very low concentration of nitrate. A MV mode appeared at VSF = 0.5–0.8 when particles are heated to 200°C. Further increasing the temperature to 300°C, all particles are in the HV mode with a VSF = 0.2–0.3, implying that most of the particles are evaporated above 300°C and particles in Cape Hedo do not contain any refractory species (e.g., BC).

Aerosol Chemical Composition

Total non-refractory PM_1 mass concentration measured by the AMS was 49.7 ± 26.5 μg m^{-3} (1.20–196.59 μg m^{-3}) in Guangzhou, and almost ten times lower (5.4 ± 3.5 μg m^{-3}, 1.1–13.3 μg m^{-3}) in Cape Hedo. Fig. 6 shows a dramatic fractional difference in chemical composition for particles in Guangzhou and in Cape Hedo. The NR-PM_1 was dominated by organics (50%), followed by sulfate (26%), nitrate (12%), ammonium and chloride (10%) in Guangzhou, comparable to another study in urban area in Hong Kong (Lee *et al.*, 2015).

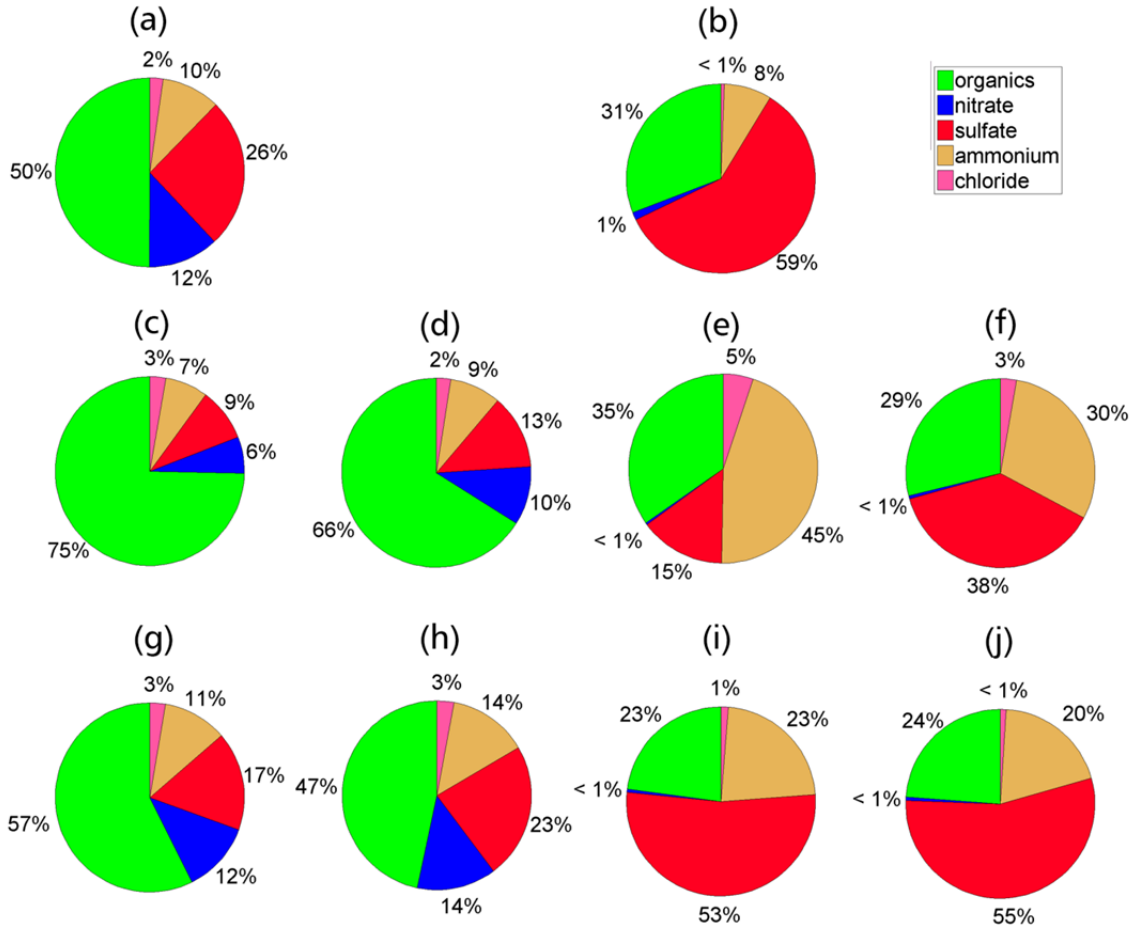

Fig. 6. The fraction chemical composition of the NR-PM_1, 110 nm, 150 nm, 200 nm and 300 nm measured by the HR-AMS in Guangzhou (a, c, d, g, h) and Cape Hedo (b, e, f, i, j).

In contrast, sulfate was the dominating species (59%) in Cape Hedo, followed by organics (31%) and ammonium (8%). Nitrate and chloride contributed less than 2% of the total, comparable to measurements made at a rural coastal site in Hong Kong (Li *et al.*, 2015). The dominant sulfate component was likely associated with cloud interaction, DMS and ship emissions in marine environment (Furutani *et al.*, 2011). For 110 and 150 nm particles (Figs. 6(c), 6(d), 6(e) and 6(f)), the chemical composition was different from the NR-PM_1 in both Guangzhou and Cape Hedo. In Guangzhou, these particles contain higher mass fraction of organics (75% and 66%), which was related to primary emission including cooking, traffic and etc. In Cape Hedo, the mass fraction of ammonium (45% and 30%) was much higher than that in NR-PM_1. The expected ammonium from the charge balance with sulfate, nitrate and chloride was much lower than the measured ammonium. It implies that these particles could contain amine (Matsumoto and Uematsu, 2005; Ooki *et al.*, 2007). For 200 and 300 nm particles, the chemical composition was similar to that in the NR-PM_1.

The mass size distribution of NR-PM_1 species resolved from the HR-ToF-AMS shows a substantial difference for particles in Guangzhou and in Cape Hedo (Fig. 7). Organics was the dominant species for all particles sizes between 50–1000 nm in Guangzhou, while sulfate was dominant in both PM_1 and accumulation mode in Cape Hedo. The high sulfate mass content in accumulation mode in Cape Hedo might be due to cloud interaction, DMS, and ship emissions in marine environments (O'Dowd *et al.*, 1997; D O'Dowd and De Leeuw, 2007; Furutani *et al.*, 2011). Fig. 7 also shows that all sulfate, organics, and ammonium components exhibit a similar mass size distribution resolved from the HR-AMS measurements, corresponding to an accumulation mode at about 310 nm, suggesting that particles in Cape Hedo are an internally mixture of the above ingredients.

Diurnal Patterns

Particle Number Size Distribution

Fig. 8 shows the diurnal variation of particle number size distribution in Guangzhou and in Cape Hedo. More dramatic variation of both particle sizes and concentrations was found in Guangzhou, indicating more complex air pollution than that in Cape Hedo. During the measurements, one and four new particle formation (NPF) events were observed in Cape Hedo and in Guangzhou respectively.

Several outbursts of particles at around 100 nm were observed in Guangzhou at around 8:00 AM and 8:00 PM, respectively (Fig. 8(a)), due to probably local traffic emissions. The number concentration of accumulation mode particles (100–1000 nm) was low at noon, probably

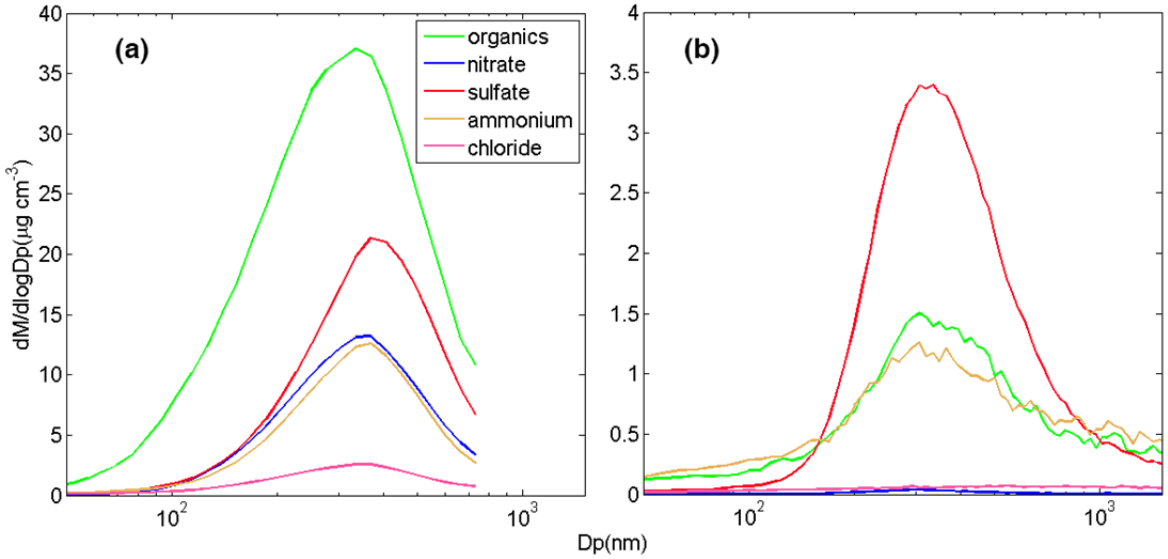

Fig. 7. The mass size distribution of the chemical composition of PM_1 measured from the HR-AMS in Guangzhou (a) and Cape Hedo (b).

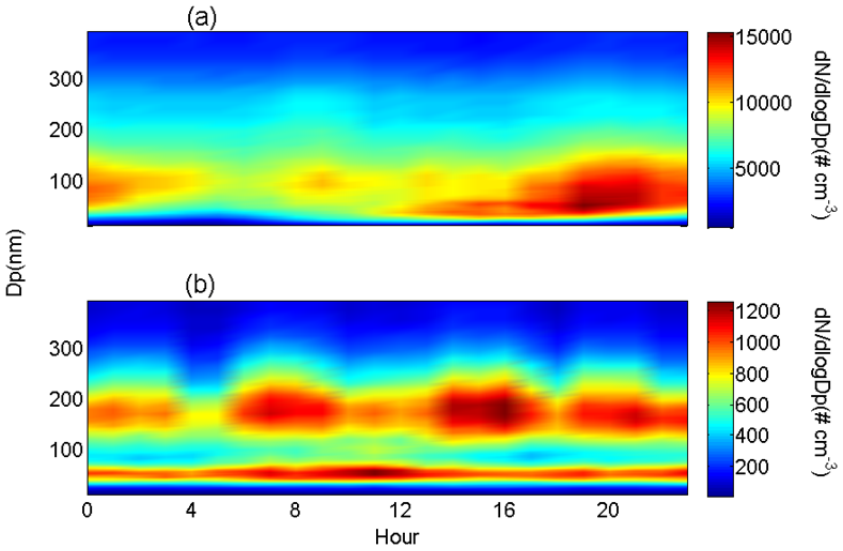

Fig. 8. Contour plots of particle number size distribution averaged over the measurement period in Guangzhou (a) and Cape Hedo (b).

because of high boundary layer, leading to dilution of the particle concentration. Meanwhile, the occurrence of smaller particles at around 20–30 nm indicates strong secondary particle formation, resulting from intensive radiation at noontime which was usually initiated at around 10 AM and subsequently grew to larger sizes during the rest of the day, large enough to potentially serve as cloud condensation nuclei (CCN) that is consistent with the results from Tan *et al.* (2016) in the PRD region.

As shown in Fig. 8(b), a bimodal distribution was clearly observed during the whole day except noontime in Cape Hedo, indicating Cape Hedo was more likely affected by the regional emissions rather than local emissions. Note that the burst of particles at around 20 nm during noontime is a typical secondary particle formation event as the particle number size distribution becomes unimodal, due to probably high solar radiation and high temperatures during noontime.

Aerosol Hygroscopicity and Volatility

Fig. 9 shows the diurnal variation of number fractions (NF_{LH}, NF_{NV}), κ_{LH}, and VSF_{mean} respectively for particles at a selected size of 150 nm as an example. Both the hygroscopicty and volatility for atmospheric particles in Guangzhou had an obvious diurnal variation. The NF_{LH}, NF_{NV} and VSF_{mean} had a small peak and the κ_{LH} reached a low level at around 9:00 AM which are associated with the low hygroscopic and low volatile species emitted from local traffic during morning rush hours. The NF_{LH}, NF_{NV}, and VSF_{mean} subsequently decreased slightly until noon, indicating an aging process for the particles. The decrease

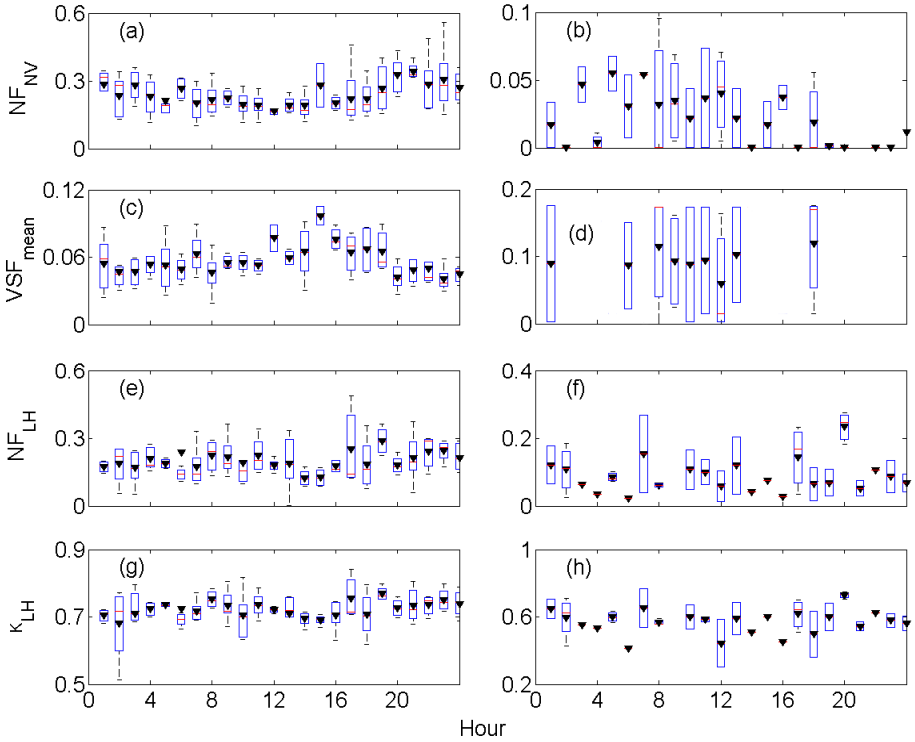

Fig. 9. The diurnal variation of NF_{LH}, NF_{NV}, κ_{mean} and VSF_{mean} for 150 nm particles averaged over the measurement period in Guangzhou (a, c, e, g) and Cape Hedo (b, d, f, h) (uncertainties are evaluated at 25% of the maximum value and 75% of the minimum value and the markers represent the mean values). The data were averaged over the measurement period whenever they were available for each hour in the 24 hour period.

of VF_{mean} suggests that particles become more volatile when aged. The mixing layer expands at noon due to heating of the atmosphere and land surface by solar radiation, leading to dilution of the particles and bringing aged particles from upper to land surface. Similarly, photochemical reactions are active during noontime to facilitate the aging process of the particles, resulting in the increase of the κ_{LH}. The NF_{LH}, NF_{NV} and VGF_{mean} increased and reached a peak at around 8:00 PM. However, the κ_{LH} stayed low in the afternoon, due to probably local traffic during evening rush hours and decreased of boundary layer height after sunset. The local pollutants are trapped in the surface layer at night, leading to a relatively high level of the NF_{LH}, NF_{NV} and VF_{mean}. In contrast, the NF_{LH}, NF_{NV}, κ_{mean} and VGF_{mean} for 150nm particles in Cape Hedo had no obvious diurnal variation during the measurement period, implying that the air was well mixed at a regional scale.

Aerosol Chemical Composition

Fig. 10 shows diurnal patterns of the measured NR-PM_1 in Guangzhou and Cape Hedo. The diurnal pattern of organics and BC in Guangzhou has a tiny peak at about 8:00 AM and a significant peak at about 8:00 PM, which is respectively associated with the rush hours in the morning and in the evening. Chloride in Guangzhou has a similar diurnal pattern to BC which could be associated with combustion including fuel, biomass and etc. Inorganic salts (nitrate, sulfate, and ammonium) in Guangzhou do not show a significant variation during the measurements, suggesting that the observed NO_3^-, SO_4^{2-}, and NH_4^+ are likely related to regional emissions. On the other hand, no obvious diurnal patterns were found for all NR-PM_1 species in Cape Hedo, implying they are formed at the regional scale.

The Relationship between Aerosol Hygroscopicity and Chemical Composition

Aerosol hygroscopicity is associated with chemical composition. The chemical composition measured by the AMS was used to calculate the hygroscopic parameter κ according to Eqs. (5–6). Fig. 11 shows the time series of the measured and calculated κ values of 110, 150 and 200 nm particles in Guangzhou and in Cape Hedo. In general, the measured κ values agreed well with the corresponding calculated κ values in Guangzhou. The average prediction biases $((\kappa_{measured} - \kappa_{calculated}/\kappa_{measured}) \times 100\%)$ fell within 10% for all sizes. The average prediction biases increased with diameter and reached 4.8% in 200nm, indicating for larger size particles the κ values were underpredicted. This discrepancy likely results from the underestimate of the hygroscopicity of organics for large size particles. With increase of the particle diameter, the organics fraction became more oxidized and more hygroscopic. This factor was not considered in the κ calculation, leading to the underestimate of the κ values. In Cape Hedo, the average prediction biases were 3.52%, 9.30% and 1.48% for 110, 150 and 200 nm, respectively. The κ values were underestimated for all particle sizes due to the underestimate fraction of organics. According to Fig. 3, the LH group was negligible indicating

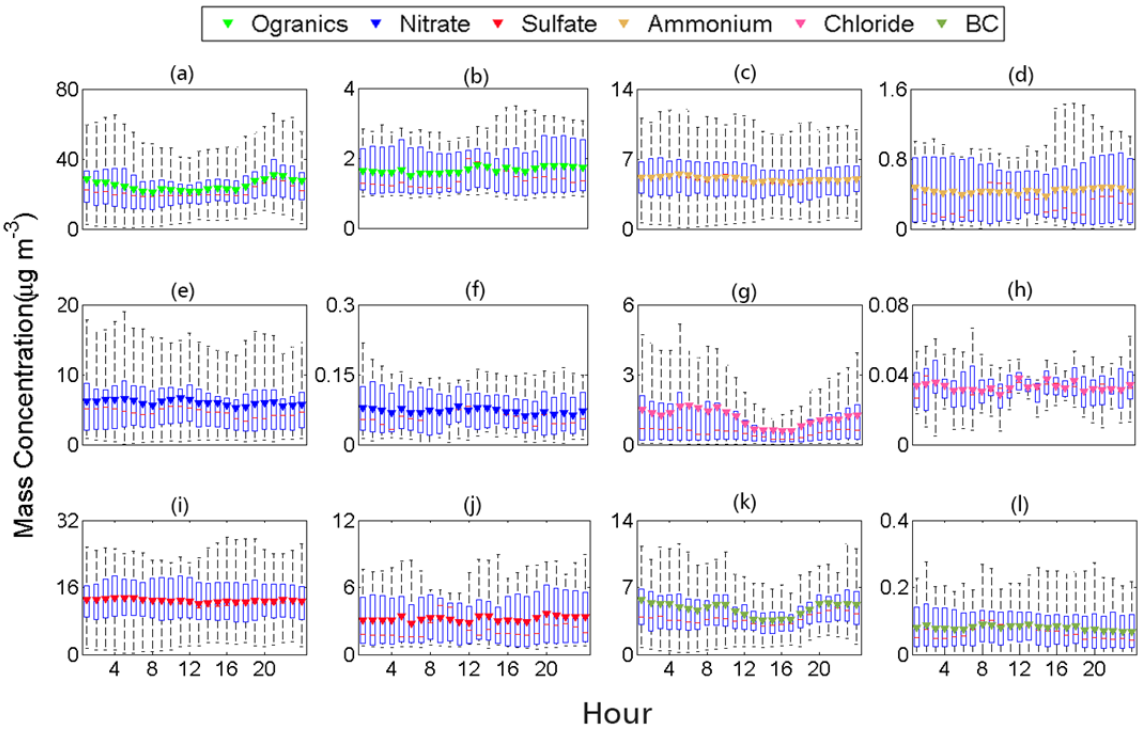

Fig. 10. The diurnal variation (25% and 75% box, maximum value and minimum value whiskers, markers is the mean) of measured NR-PM_1 species (organics, nitrate, sulfate, ammonium, chloride and BC) averaged over the measurement period in Guangzhou (a, c, e, g, i, k) and Cape Hedo (b, d, f, h, j, l).

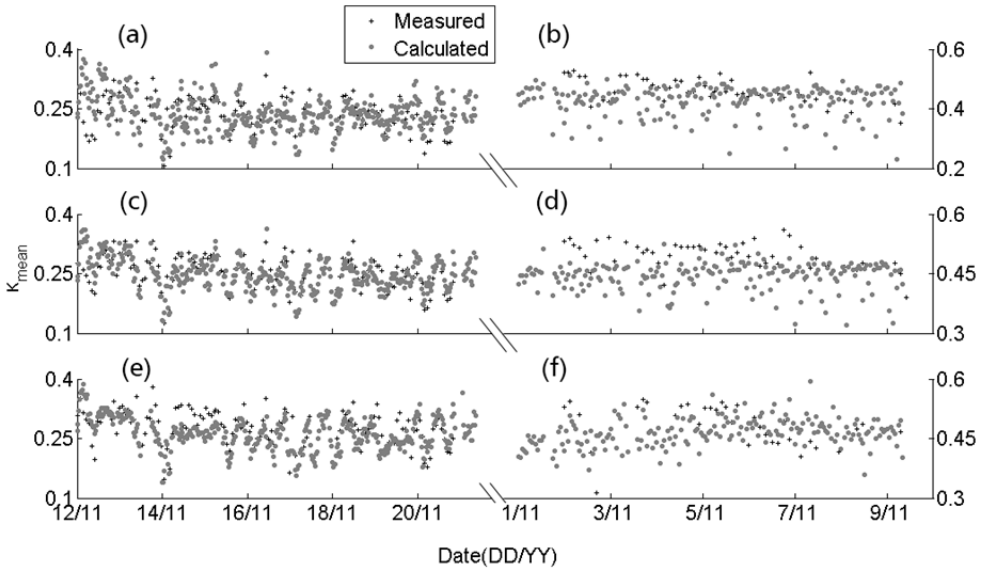

Fig. 11. The timeseries of measured κ_{mean} and calculated κ_{mean} for 110, 150 and 200 nm particles in Guangzhou (a, c, e) and Cape Hedo (b, d, f).

that the organics was aged and oxidized, mixed with other compounds, leading to higher hygroscopic than the assumed value ($\kappa = 0.1$). In addition, sufficient ammonium could form other inorganic salts, which are not considered in our ion paring scheme, hence result in higher aerosol hygroscopicity.

Aerosol Mixing State and Source Origin

The physical and chemical properties (hygroscopicity, volatility, mixing state, and chemical composition) of atmospheric particles are dependent on the air mass origin. We performed backward trajectory modeling to investigate the relationship between air masses and the variation of the aerosol properties using NOAA HYSPLIT4.0. Air mass trajectories were modeled backward 72 hours and air mass history was classified according to cluster analysis. We focused on accumulation mode particles since they are more

representative of aerosol transport than smaller particles. We hence chose three sizes of particles (110 nm, 150 nm and 200 nm) in our discussion.

The trajectories were classified into five and three clusters for air masses at the Panyu site in Guangzhou and at the Cape Hedo site in Okinawa, respectively, based on the backward trajectory modeling (Fig. 12). The Panyu site was mainly affected by air masses originated from North (Clusters 1, 2, 3 in Fig. 12(a)), East (Cluster 4 in Fig. 12(a)), and Southeast (Cluster 5 in Fig. 12(a)), while the Cape Hedo site was affected by those from North (Clusters 1 in Fig. 12(b)), East (Cluster 2 in Fig. 12(b)), and Southeast (Cluster 3 in Fig. 12(b)).

Air masses at the Panyu site reside longer in Clusters 1 and 2 than in other clusters below 500 meter. The particles that were constrained in the mixing layer were susceptible to more aging process than those in the upper level due to higher concentrations of gaseous pollutants and moisture content in the mixing layer (Zhang *et al.*, 2015). More aged particles were found for air masses in clusters 1 and 2 as indicated by a lower value of the NF_{LH} and NF_{NV} than those in other clusters (Fig. 13). On the other hand, air masses in Cluster 3 at the Cape Hedo site stayed shorter in the mixing layer, leading to less aged particles as indicated by a lower level of the corresponding NF_{LH} and NF_{NV}.

CONCLUSION

In this paper, H/V-TDMA and AMS were used to measure aerosol hygroscopicity, volatility and chemical composition in Guangzhou and Cape Hedo in November, respectively. The Guangzhou site and the Cape Hedo site were used to study the aerosol properties in urban environment and marine environment, respectively.

In general, the particle number size distribution showed multimodal distribution in Guangzhou, while the PNSD in Cape Hedo tended to show bimodal distribution, demonstrating that particles in urban origin from more complex local emissions than those in Cape Hedo. The N_{CN} in Guangzhou was about 10 times that in Cape Hedo, indicating that urban environments suffered heavier pollution than marine environments.

The κ_{mean} of 40–200 nm particles in marine environment ranged from 0.48 to 0.52, while the κ_{mean} in urban environments ranged from 0.22 to 0.31. The H/V-TMDA measurements show that the number fraction of LH and NV in Cape Hedo was far lower than in Guangzhou, suggesting that the impact of local anthropogenic emissions was lower in the marine site. Particles in marine environments tended to be internally mixed, while particles in urban are externally mixed to a higher extent. The difference of volatility at different temperatures reflects the difference in the chemical composition in Cape Hedo and Guangzhou, as also measured by AMS.

The AMS measurement shows that the NR-PM_1 was dominant by organics in Guangzhou, which was associated with local anthropogenic emissions including traffic, cooking, etc. While sulfate was the dominant species in Cape Hedo, the size-resolved chemical composition indicates that sulfate might be associated with cloud interaction, DMS and ship emissions in marine environments.

An analysis of diurnal variation in PNSD shows that NPF occurred both in Guangzhou and in Cape Hedo at noon, and the aging process was also measured at noon. The smooth diurnal variation in Cape Hedo indicates that the site was rarely affected by local emissions. The local traffic emissions in urban could lead to the two peaks at about 100 nm in the morning and evening. It was also associated with the variation of hygroscopicity, volatility and chemical composition.

The κ value calculated based on chemical composition agreed well with the measurements in Guangzhou. The κ values were both underpredicted in Guangzhou and Cape Hedo, which could result from the underestimate of the hygroscopicity of aged organics.

Back trajectory cluster analysis shows that the air masses arriving in Guangzhou and Cape Hedo could be classified into five and three clusters, respectively. It also demonstrates that the aged particles have closely correlated with the times the air masses stay in the boundary layer.

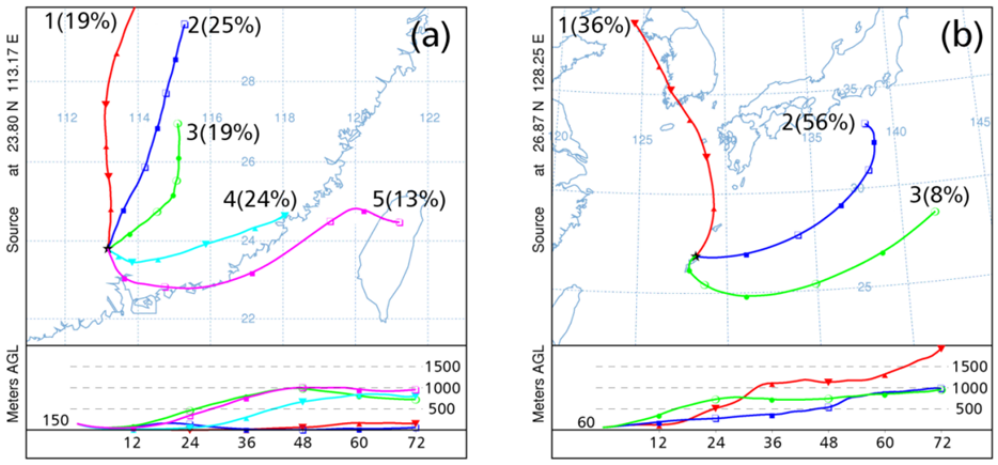

Fig. 12. The 72 hour backward trajectory modeling for simulating air masses that arrived at the Panyu site (a) and at the Cape Hedo site (b).

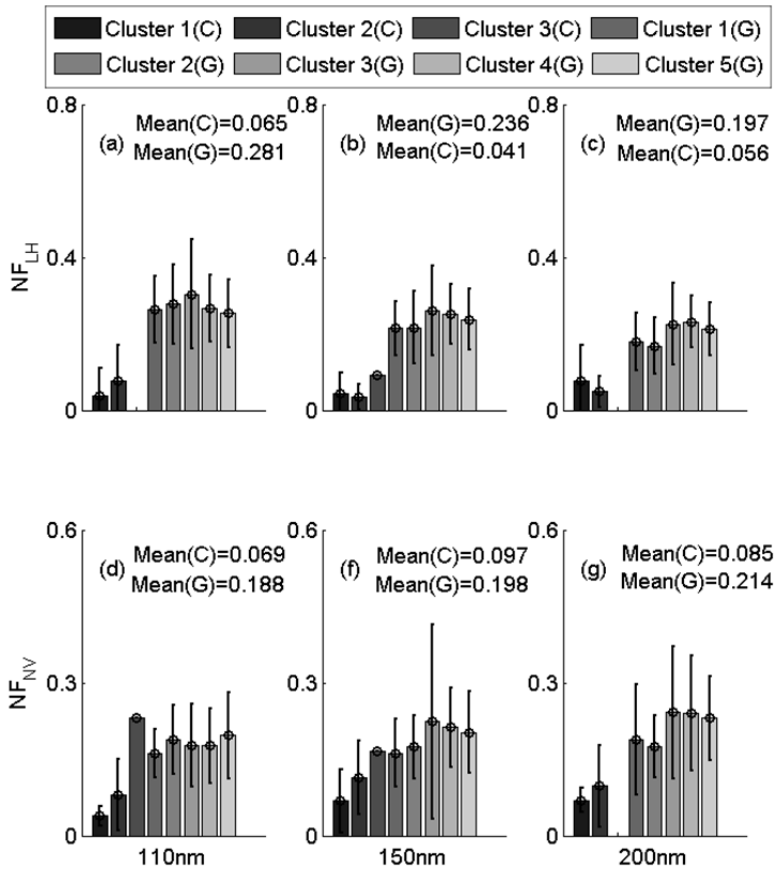

Fig. 13. Average number fraction (NF) of NV (300°C) and LH particles for six measured diameters based on the classified clusters. C represents Cape Hedo and G represents Guangzhou.

ACKNOWLEDGEMENTS

The authors would like to acknowledge supports from National Key Project of MOST (2016YFC0201901), Special R&D fund for research institutes (2014EG137243), Natural Science Foundation of China (41375156, 21577177) and Guangdong provincial scientific planning project (2014A020216008).

REFERENCE

Allan, J.D., Alfarra, M.R., Bower, K.N., Coe, H., Jayne, J.T., Worsnop, D.R., Aalto, P.P., Kulmala, M., Hyötyläinen, T. and Cavalli, F. (2006). Size and composition measurements of background aerosol and new particle growth in a Finnish forest during QUEST 2 using an Aerodyne Aerosol Mass Spectrometer.. *Atmos. Chem. Phys.* 6: 315–327.

Bardouki, H., Liakakou, H., Economou, C., Sciare, J., Smolık, J., Ždímal, V., Eleftheriadis, K., Lazaridis, M., Dye, C. and Mihalopoulos, N. (2003). Chemical composition of size-resolved atmospheric aerosols in the eastern Mediterranean during summer and winter. *Atmos. Environ.* 37: 195–208.

Cavalli, F., Facchini, M., Decesari, S., Emblico, L., Mircea, M., Jensen, N. and Fuzzi, S. (2006). Size-segregated aerosol chemical composition at a boreal site in southern Finland, during the QUEST project. *Atmos. Chem. Phys.* 6: 993–1002.

Chan, C.K. and Yao, X. (2008). Air pollution in mega cities in China. *Atmos. Environ.* 42: 1–42.

Cheung, H.H., Tan, H., Xu, H., Li, F., Wu, C., Yu, J.Z. and Chan, C.K. (2016). Measurements of non-volatile aerosols with a VTDMA and their correlations with carbonaceous aerosols in Guangzhou, China. *Atmos. Chem. Phys.* 16: 8431–8446.

Decarlo, P.F., Kimmel, J.R., Achim, T., Northway, M.J., Jayne, J.T., Aiken, A.C., Marc, G., Katrin, F., Thomas, H. and Docherty, K.S. (2006). Field-deployable, high-resolution, time-of-flight aerosol mass spectrometer. *Anal. Chem.* 78: 8281–8289.

Dusek, U., Frank, G.P., Hildebrandt, L., Curtius, J., Schneider, J., Walter, S., Chand, D., Drewnick, F., Hings, S., Jung, D., Borrmann, S. and Andreae, M.O. (2006). Size matters more than chemistry for cloud-nucleating ability of aerosol particles. *Science* 312: 1375–1378.

Furutani, H., Jung, J., Miura, K., Takami, A., Kato, S., Kajii, Y. and Uematsu, M. (2011). Single-particle chemical characterization and source apportionment of iron-containing atmospheric aerosols in Asian outflow. *J. Geophys. Res.* 116: 597–616.

Gysel, M., Crosier, J., Topping, D.O., Whitehead, J.D., Bower, K.N., Cubison, M.J., Williams, P.I., Flynn, M.J., McFiggans, G.B. and Coe, H. (2007). Closure study between chemical composition and hygroscopic growth

of aerosol particles during TORCH2. *Atmos. Chem. Phys.* 7: 6131–6144.

Heintzenberg, J., Covert, D. and Van Dingenen, R. (2000). Size distribution and chemical composition of marine aerosols: A compilation and review. *Tellus B* 52: 1104–1122.

Jimenez, J.L., Jayne, J.T., Shi, Q., Kolb, C.E., Worsnop, D.R., Yourshaw, I., Seinfeld, J.H., Flagan, R.C., Zhang, X. and Smith, K.A. (2003). Ambient aerosol sampling using the Aerodyne Aerosol Mass Spectrometer. *J. Geophys. Res.* 108: 8425.

Lee, B.P., Li, Y.J., Yu, J.Z., Louie, P.K. and Chan, C.K. (2015). Characteristics of submicron particulate matter at the urban roadside in downtown Hong Kong—Overview of 4 months of continuous high-resolution aerosol mass spectrometer measurements. *J. Geophys. Res.* 120: 7040–7058.

Li, L., Wang, W., Feng, J., Zhang, D., Li, H., Gu, Z., Wang, B., Sheng, G. and Fu, J. (2010). Composition, source, mass closure of $PM_{2.5}$ aerosols for four forests in eastern China. *J. Environ. Sci.* 22: 405–412.

Li, Y., Lee, B.P., Su, L., Fung, J.C.H. and Chan, C.K. (2015). Seasonal characteristics of fine particulate matter (PM) based on high-resolution time-of-flight aerosol mass spectrometric (HR-ToF-AMS) measurements at the HKUST Supersite in Hong Kong. *Atmos. Chem. Phys.* 15: 37–53.

Li, Y.J., Sun, Y.L., Zhang, Q., Li, X., Li, M., Zhou, Z., and Chan, C.K. (2017). Real-time chemical characterization of atmospheric particulate matter in China: A review. *Atmos. Environ.* 158: 270–304.

Liu, P.F., Zhao, C.S., Göbel, T., Hallbauer, E., Nowak, A., Ran, L., Xu, W.Y., Deng, Z.Z., Ma, N., Mildenberger, K., Henning, S., Stratmann, F. and Wiedensohler, A. (2011). Hygroscopic properties of aerosol particles at high relative humidity and their diurnal variations in the North China Plain. *Atmos. Chem. Phys.* 11: 3479–3494.

Matsumoto, K. and Uematsu, M. (2005). Free amino acids in marine aerosols over the western North Pacific Ocean. *Atmos. Environ.* 39: 2163–2170.

Meng, J.W., Yeung, M.C., Li, Y.J., Lee, B.Y.L. and Chan, C.K. (2014). Size-resolved cloud condensation nuclei (CCN) activity and closure analysis at the HKUST Supersite in Hong Kong. *Atmos. Chem. Phys*. 14: 10267–10282.

Mochida, M., Nishita-Hara, C., Kitamori, Y., Aggarwal, S.G., Kawamura, K., Miura, K. and Takami, A. (2010). Size-segregated measurements of cloud condensation nucleus activity and hygroscopic growth for aerosols at Cape Hedo, Japan, in spring 2008. *J. Geophys. Res.* 115: D21207.

Ooki, A., Uematsu, M. and Noriki, S. (2007). Size-resolved sulfate and ammonium measurements in marine boundary layer over the North and South Pacific. *Atmos. Environ*. 41: 81–91.

Petters, M. and Kreidenweis, S. (2007). A single parameter representation of hygroscopic growth and cloud condensation nucleus activity. *Atmos. Chem. Phys.* 7: 1961–1971.

Qin, Y.M., Tan, H.B., Li, Y.J., Schurman, M.I., Li., F., Canonaco, F., Prévôt, A.S.H. and Chan, C.K. (2017). The role of traffic emissions in particulate organics and nitrate at a downwind site in the periphery of Guangzhou, China. *Atmos. Chem. Phys.* 17: 10245–10258.

Randall, D.A., Solomon, S., Qin, D., Manning, M., Chen, Z., Tignor, M., Marquis, M., Avervt, K.B. and Miller, H.L. (2007). *Climate models and their evaluation*. Cambridge University Press, Cambridge,UK.

Stocker, D.Q. (2013). *Climate change 2013: The Physical science basis*. Working Group I Contribution to the Fifth Assessment Report of the Intergovernmental Panel on Climate Change, Summary for Policymakers, IPCC.

Stokes, R. and Robinson, R. (1966). Interactions in aqueous nonelectrolyte solutions. I. Solute-solvent equilibria. *J. Phys. Chem.* 70: 2126–2131.

Stolzenburg, M.R. and McMurry, P.H. (2008). Equations governing single and tandem dma configurations and a new lognormal approximation to the transfer function. *Aerosol Sci. Technol.* 42: 421–432.

Swietlicki, E., Hansson, H.C., HÄMeri, K., Svenningsson, B., Massling, A., McFiggans, G., McMurry, P.H., PetÄJÄ, T., Tunved, P., Gysel, M., Topping, D., Weingartner, E., Baltensperger, U., Rissler, J., Wiedensohler, A. and Kulmala, M. (2008). Hygroscopic properties of submicrometer atmospheric aerosol particles measured with H-TDMA instruments in various environments—A review. *Tellus B* 60: 432–469.

Tan, H., Yin, Y., Gu, X., Li, F., Chan, P.W., Xu, H., Deng, X. and Wan, Q. (2013a). An observational study of the hygroscopic properties of aerosols over the Pearl River Delta region. *Atmos. Environ.* 77: 817–826.

Tan, H., Xu, H., Wan, Q., Li, F., Deng, X., Chan, P.W., Xia, D. and Yin, Y. (2013b). Design and application of an unattended multifunctional H-TDMA system. *J. Atmos. Ocean. Technol.* 30: 1136–1148.

Tao, J., Zhang, L., Engling, G., Zhang, R., Yang, Y., Cao, J., Zhu, C., Wang, Q. and Luo, L. (2013). Chemical composition of $PM_{2.5}$ in an urban environment in Chengdu, China: Importance of springtime dust storms and biomass burning. *Atmos. Res.* 122: 270–283.

Topping, D.O., McFiggans, G.B. and Coe, H. (2005). A curved multi-component aerosol hygroscopicity model framework: Part 1 – Inorganic compounds. *Atmos. Chem. Phys.* 5: 1205–1222.

Wang, X., Bi, X., Sheng, G. and Fu, J. (2006). Chemical composition and sources of PM_{10} and $PM_{2.5}$ aerosols in Guangzhou, China. *Environ. Monit. Assess.* 119: 425–439.

Wehner, B., Philippin, S., Wiedensohler, A., Scheer, V. and Vogt, R. (2004). Variability of non-volatile fractions of atmospheric aerosol particles with traffic influence. *Atmos. Environ.* 38: 6081–6090.

Wehner, B., Berghof, M., Cheng, Y.F., Achtert, P., Birmili, W., Nowak, A., Wiedensohler, A., Garland, R.M., Pöschl, U., Hu, M. and Zhu, T. (2009). Mixing state of nonvolatile aerosol particle fractions and comparison with light absorption in the polluted Beijing region. *J. Geophys. Res.* 114: D00G17.

Yang, H., Yu, J.Z., Ho, S.S.H., Xu, J., Wu, W.-S., Wan, C.H., Wang, X., Wang, X. and Wang, L. (2005). The chemical composition of inorganic and carbonaceous materials in $PM_{2.5}$ in Nanjing, China. *Atmos. Environ.* 39: 3735–3749.

Ye, B., Ji, X., Yang, H., Yao, X., Chan, C.K., Cadle, S.H., Chan, T. and Mulawa, P.A. (2003). Concentration and chemical composition of $PM_{2.5}$ in Shanghai for a 1-year period. *Atmos. Environ.* 37: 499–510.

Ye, X., Ma, Z., Hu, D., Yang, X. and Chen, J. (2011). Size-resolved hygroscopicity of submicrometer urban aerosols in Shanghai during wintertime. *Atmos. Res.* 99: 353–364.

Yeung, M.C., Lee, B.P., Li, Y.J. and Chan, C.K. (2014). Simultaneous HTDMA and HR-ToF-AMS measurements at the HKUST Supersite in Hong Kong in 2011. *J. Geophys. Res.* 119: 9864–9883.

Zdanovskii, A. (1948). Novyi metod rascheta rastvorimostei elektrolitov v mnogokomponentnykh sistemakh. 1. *Zhurnal Fizicheskoi Khimii* 22: 1478–1485.

Zhang, S.L., Ma, N., Kecorius, S., Wang, P.C., Hu, M., Wang, Z.B., Größ, J., Wu, Z.J. and Wiedensohler, A. (2015). Mixing state of atmospheric particles over the North China Plain. *Atmos. Environ.* 125: 152–164.

Received for review, January 11, 2017
Revised, April 15, 2017
Accepted, April 16, 2017